



ISSN (Print) : 2320 – 3765
ISSN (Online): 2278 – 8875

International Journal of Advanced Research in Electrical, Electronics and Instrumentation Engineering

(A High Impact Factor & UGC Approved Journal)

Website: www.ijareeie.com

Vol. 6, Issue 9, September 2017

Comparative Study on Octagonal Photonic Crystal Fiber with Different Air Holes for Supercontinuum Generation

Aparna A Nair¹, M.Jayaraju²

Department of Electronics and Communication Engineering, College of Engineering Trivandrum, Kerala, India¹

MES Institute of Technology and Management, Kollam, Kerala, India²

ABSTRACT: In this work a comparative study is made on supercontinuum generation in octagonal photonic crystal fiber (O-PCF) with circular air holes and O-PCF with elliptical air holes. Supercontinuum generation is investigated in each designed O-PCF and with femtosecond optical pulses of 50 fs at 830 nm for pump power of 10 kW obtained SC spectrum of wavelength ranges from 580 nm- 1200nm.

KEYWORDS: Photonic crystal fiber, Supercontinuum generation, Birefringence, Dispersion coefficient.

I.INTRODUCTION

Photonic crystal fibers consisting of a central defect region in a regular lattice of air holes have attracted many recent applications due to its flexibility in design. The photonic crystal fiber has been realized by introducing air holes of different shapes (like circular, elliptical etc.) arranged in certain lattice pattern (like hexagon, octagon etc.) around the solid pure silica material and running along the entire fiber length [1]. By varying the air hole size and shape, it is possible to obtain unique features like low confinement losses, zero dispersion at desired wavelength, ultra-flattened chromatic dispersion, endlessly single mode and so on. It attracts much attention in various applications in such diverse fields as pulse compression, spectroscopy, biomedical applications, supercontinuum (SC) generation which can be used as a source to create multi-wavelength optical sources for wavelength division multiplexing (WDM), optical communication systems and so on. Many novel designs like, hexagonal ring [2], square lattice [3], circular ring [4], octagonal lattice, PCF with elliptical air holes [5], PCF with square air holes [6] are being introduced to realize these unique properties based on the requirement of the applications. Comparing with hexagonal lattice PCF, non-hexagonal lattice like octagonal lattice has reported with many attractive features such as low confinement loss, smaller effective area, highly nonlinear, and wideband single-mode operation. This is mainly due to the presence of more number of air holes in a single ring than a hexagonal lattice ring does [7].

One of the most advancing research on PCF is supercontinuum generation in under different photonic crystal fibers due to its numerous applications in the field of optical communication [8] and medical applications [9]. There are many nonlinear processes like self-phase modulation (SPM), four wave mixing (FWM), modulational instability, self-steepening, stimulated Raman scattering (SRS), soliton fission and so on results in the generation of SC over a wide wavelength range [10]. M.A. Hossain *et al* [11] have presented theoretical calculation of a highly nonlinear germanium doped photonic crystal fiber with all-normal group velocity dispersion to design a SC light source at 1.55 μm for medical and optical communication applications. In 2006 J.M. Dudley *et al* [12] have described evolution of SC and explained in detail the effect of pulse duration, pump power and all the nonlinear processes involved in the SC generation. Recently Wang *et al* [13] experimentally demonstrated ultraviolet and visible SCs are efficiently generated from 180 to 1100 nm based on the higher-order modes of PCF using Ti:Sapphire laser with centre wavelength of 790 nm. Also, Xu *et al* [14] have demonstrated square lattice PCF generated SC spectrum ranging from 1500 nm to 1800 nm with a pump power of 6 W. Due to dispersive properties of PCF, it is found to be a good choice for supercontinuum generation. A A Nair *et al* [15] have studied supercontinuum generation in O-PCF with a combination of circular and elliptical air holes and achieved SC spectrum ranging from 700 nm-11500 nm. Later M. Rashid *et al* [16] have

International Journal of Advanced Research in Electrical, Electronics and Instrumentation Engineering

(A High Impact Factor & UGC Approved Journal)

Website: www.ijareeie.com

Vol. 6, Issue 9, September 2017

demonstrated O-PCF with high birefringence 2.04×10^{-2} with nonlinear coefficient of $33 \text{ W}^{-1} \text{ km}^{-1}$ at 1550 nm suitable for supercontinuum generation.

In this work we focussed on the supercontinuum generation in the proposed PCF with elliptical air holes and circular air holes. We carried out the simulation using MATLAB software for supercontinuum generation using split step Fourier transform. The different PCF designs proposed are O-PCF with circular air holes of radius (i) $R_{C1} = 0.6 \mu\text{m}$, (ii) $R_{C2} = 0.4 \mu\text{m}$ and O-PCF with elliptical air holes of major axis radius of (iii) $R_e = 0.4 \mu\text{m}$. SC spectrum generated for each proposed design and compared result of each design.

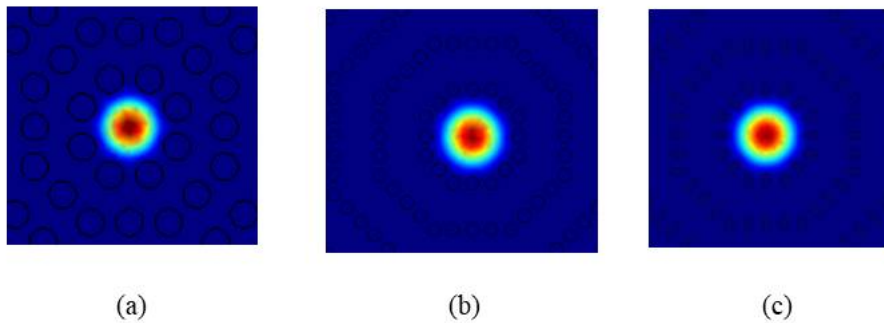


Fig.1 Typical mode pattern of the O-PCF with circular air hole radius of (a) $R_{C1} = 0.6 \mu\text{m}$ (b) $R_{C2} = 0.4 \mu\text{m}$ and elliptical air hole radius of (c) $R_e = 0.4 \mu\text{m}$ at 1000 nm .

II. THEORY AND DESIGN

Supercontinuum or white light generation is a phenomenon arises when high intensity monochromatic optical pulses passes through a nonlinear medium like highly nonlinear PCF generates an output of pulses of broad spectral bandwidth. This process results due to various nonlinear process like self-focusing, stimulated Raman effect, self-steepening, four wave mixing, stimulated Brillouin scattering, self-phase modulation (SPM), cross phase modulation (XPM) and so on [12]. The nonlinear phenomenon dominates for the spectral broadening is determined by the dispersive properties of the medium, pulse width, center wavelength of the laser etc. For example, in case femtosecond SC generation, four wave mixing and modulation instability plays important role in initial broadening of the spectrum. The propagation of optical wave through an optical medium is generally governed by Nonlinear Schrodinger equation (NLSE) is given by [17],

$$\frac{\partial}{\partial z} A(z, T) = -\frac{\alpha(\omega)}{2} A(z, T) + \sum_{n \geq 2} \beta_n \frac{i^{n+1}}{n!} \frac{\partial^n}{\partial t^n} A(z, T) + i\gamma \left(+ \frac{i}{\omega_0} \frac{\partial}{\partial T} \int_{-\infty}^{\infty} R(T') |A(z, -T')|^2 dT' \right) \quad (1)$$

This equation represents the propagation of optical pulse through the fiber where $A(z, T)$ is the electric field envelop α is the frequency dependent loss, β_n is the n^{th} order dispersion at center frequency ω_0 and $R(T)$ is the Raman response function. The Raman response is defined as $R(T) = (1 - f_r)\delta(T) + f_r h_r$, for silica $f_r = 0.18$ and $h_r(T) = \frac{\tau_1^2 + \tau_2^2}{\tau_1 \tau_2^2} e^{-\frac{T}{\tau_1}} \sin\left(-\frac{T}{\tau_1}\right)$, $\tau_1 = 12.2 \text{ fs}$, $\tau_2 = 32 \text{ fs}$ [18]. This equation is solved using split step Fourier transform method which is simple and accurate. The NLSE equation is solved in taking account of dispersive and nonlinear effects separately for very small step dz . The optical pulse used is of hyperbolic secant pulse profile which is given as,

$$A(z, T) = \sqrt{P_0} \text{sech} \left(\frac{T}{T_0} \right) \quad (2)$$

Where P_0, T_0 are peak power and pulse width of the input pulse respectively. When a pulse with sufficient peak power breaks up into a series of lower-amplitude sub pulses is termed as soliton fission [12]. The soliton order of the input pulse N is determined by both pulse and fiber parameters through is given by,

$$N = L_D / L_{NL} \quad (3)$$

where L_D is the dispersive length and L_{NL} is the nonlinear length.

The finite element method (FEM) with rectangular perfectly matched boundary layers (PML) is used to simulate each properties of the PCF. In order to obtain each photonic crystal fiber parameter, it is important to calculate the effective refractive index of the cladding. Fig.1 shows the modal intensity distribution of proposed O-PCF with circular air holes of radius $R_{c1}=0.6 \mu\text{m}$, $R_{c2} = 0.4 \mu\text{m}$ and elliptical air hole radius of $R_e = 0.4 \mu\text{m}$. Effective refractive index represents the phase delay per unit length in a waveguide. An effective refractive index for single mode fiber is also known as phase index or normalized phase change coefficient. The modal effective refractive indexes are solved from Maxwell's equations and given by,

$$n_{\text{eff}} = \frac{\beta}{k_0} \quad (4)$$

Where β is the propagation constant and k_0 is the free space wave number.

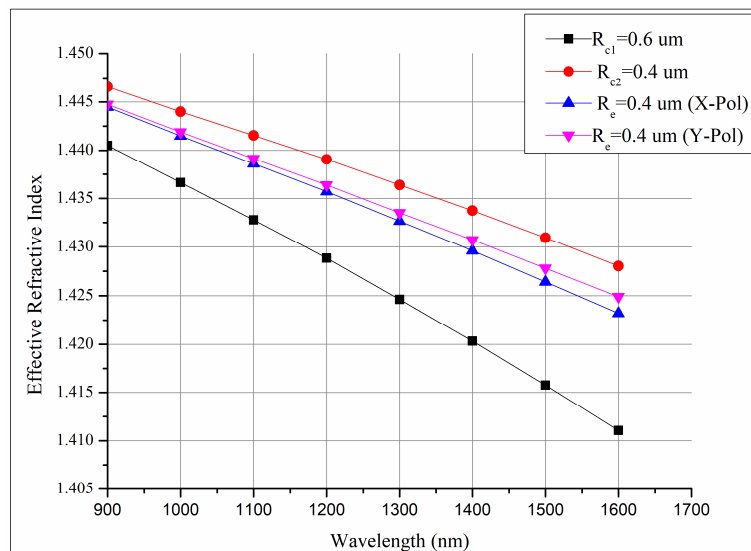


Fig:2 Effective Refractive index as a function of wavelength for each proposed design of O-PCF with circular air hole radius of $R_{c1}=0.6 \mu\text{m}$, $R_{c2} = 0.4 \mu\text{m}$ and elliptical air hole radius of $R_e = 0.4 \mu\text{m}$.

III. RESULT AND DISCUSSION

Fig.2 shows the variation of effective refractive index with wavelength ranges from 900nm-1600 nm. The plot shows that the effective refractive depends on the air hole size and which is found to inversely proportional to the radius of the air hole. There is a drastic change due to the size of air holes in effective refractive from the refractive index of its base material, ie silica. For elliptical air holes there will be two refractive indices based on the polarisation (X-polarisation and Y-polarisation) which is plotted in the fig.2. Fig.3 (a), 3 (b) and 3 (c) shows the SC spectra of each proposed O-PCF of radius $R_{C1}=0.6 \mu\text{m}$, $R_{C2} = 0.4 \mu\text{m}$ and $R_e = 0.4 \mu\text{m}$ (X-polarisation) for pulse width of 50 fs and pump power of 10 kW at 830 nm wavelength. In fig.3 (a) the optical parameters like nonlinear coefficient is of $38 \text{ W}^{-1}\text{km}^{-1}$, second order dispersion $\beta_2 = -0.01363 \text{ ps}^2/\text{m}$, for Fig.3 (b) nonlinear coefficient is of $27 \text{ W}^{-1}\text{km}^{-1}$, second order dispersion $\beta_2 = -0.3104 \text{ ps}^2/\text{m}$, and fig.3 (c) nonlinear coefficient is of $23 \text{ W}^{-1}\text{km}^{-1}$, pump power 10 kW, second order dispersion $\beta_2 = -0.1218 \text{ ps}^2/\text{m}$ and thus the soliton order for each design found to be $N=10,6,6$ using equation.3 respectively. The SC spectrum expands approximately from 580 nm-1200 nm, so nearly 620 nm bandwidth is achieved for PCF will circular air holes of radius $R_{C1}= 0.6 \mu\text{m}$ whereas PCF with circular air holes of radius $R_{C2} = 0.4 \mu\text{m}$ SC expands from 580 nm - 1100 nm so approximately 520 nm which is also found to be same for the SC spectrum of PCF with elliptical air

International Journal of Advanced Research in Electrical, Electronics and Instrumentation Engineering

(A High Impact Factor & UGC Approved Journal)

Website: www.ijareeie.com

Vol. 6, Issue 9, September 2017

holes. In femtosecond regime, pulse width of 50 fs Raman and higher order dispersion introduces perturbation which leads to soliton fission[12]. It is clear that as the soliton order, N increases the bandwidth of the generated SC also increases.

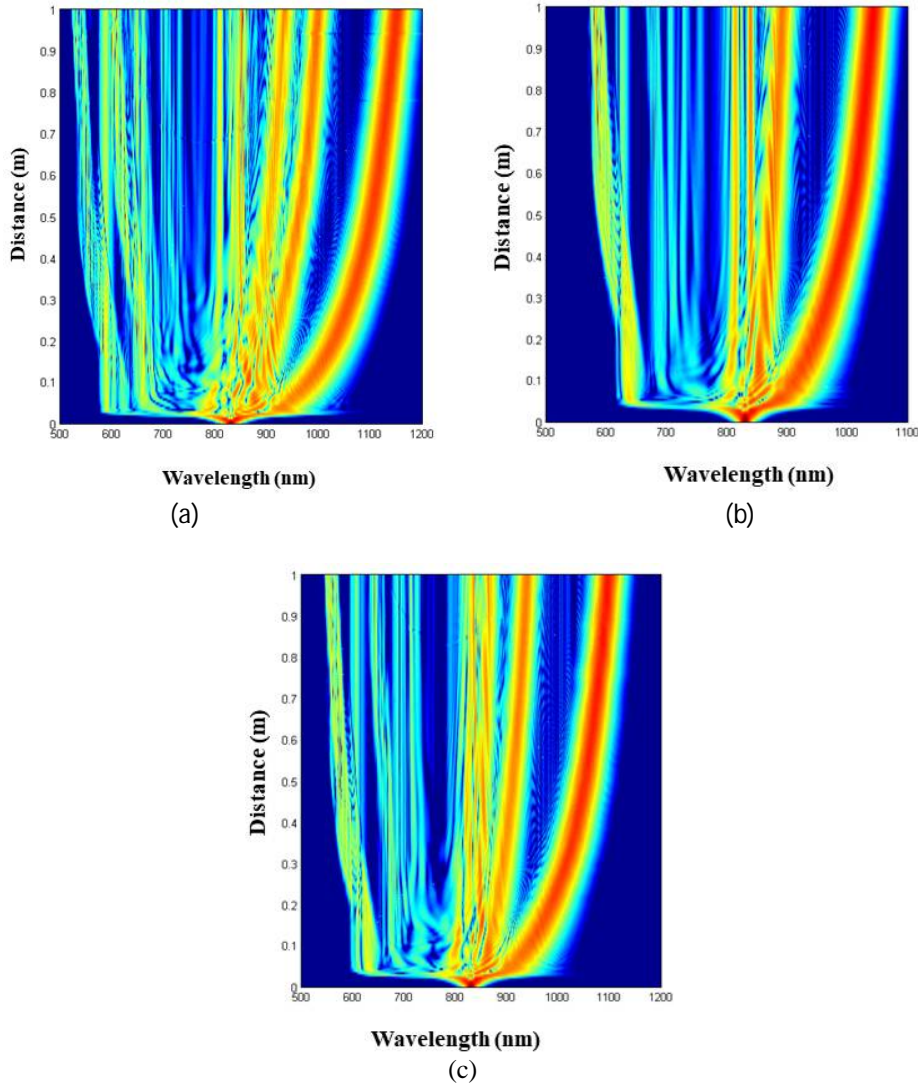


Fig.3 Spectral evolutions of the supercontinuum generated by proposed PCF of pump power of 10 kW and pulse duration 50fs at 830 nm wavelength for (a) circular air hole of radius $R_{C1} = 0.6 \mu\text{m}$ (b) circular air hole of radius $R_{C2} = 0.4 \mu\text{m}$ and (c) elliptical air holes of radius $R_e = 0.4 \mu\text{m}$.

IV. CONCLUSION

In this investigation we studied and compared O-PCF with circular and O-PCF with elliptical air holes by varying radius of air holes. The SC generation is obtained using a pump power of 10 kW for pulse width of 50 fs is applied to each proposed design at 830 nm. It is observed that O-PCF with circular air hole of radius $R_{C1} = 0.6 \mu\text{m}$ produced a SC spectrum of wavelength ranging from 580nm-1200nm which is found to be broad comparing with other two designs. O-PCF with circular air hole of radius $R_{C2} = 0.4 \mu\text{m}$ and O-PCF with elliptical air holes have same soliton order and thus it is observed that the bandwidth of SC spectrum of both O-PCF with circular air holes and O-PCF with elliptical



ISSN (Print) : 2320 – 3765
ISSN (Online): 2278 – 8875

International Journal of Advanced Research in Electrical, Electronics and Instrumentation Engineering

(A High Impact Factor & UGC Approved Journal)

Website: www.ijareeie.com

Vol. 6, Issue 9, September 2017

air holes found to be same. This broadband and highly efficient SC generation finds extensive applications for the ultrafast for many ultrafast and optical communication applications.

REFERENCES

- [1] P.S.J. Russell, Photonic-crystal fibers, *J. Light. Technol.* 24 (2006) 4729–4749..
- [2] J.K. Ranka, R.S. Windeler, A.J. Stentz, Optical properties of high-delta air – silica microstructure optical fibers, *Opt. Lett.* 25 (2000) 796–798.
- [3] B. Dabas, R.K. Sinha, Dispersion characteristic of hexagonal and square lattice chalcogenide As₂Se₃ glass photonic crystal fiber, *Opt. Commun.* 283 (2010) 1331–1337.
- [4] C.S. Kumar, R. Anbazhagan, Investigation on chalcogenide and silica based photonic crystal fibers with circular and octagonal core, *AEU - Int. J. Electron. Commun.* 72 (2017) 40–45.
- [5] J. Liao, J. Sun, High birefringent rectangular-lattice photonic crystal fibers with low confinement loss employing different sizes of elliptical air holes in the cladding and the core, *Opt. Fiber Technol.* 18 (2012) 457–461.
- [6] A. Medjouri, L. Simohamed, O. Ziane, A. Boudrioua, Investigation Of High Birefringence And Chromatic Dispersion Management In Photonic Crystal Fiber With Square Air Holes, *Optik*, 126 (2015) 2269–2274.
- [7] S.M. Habib, M.S. Habib, M.I. Hasan, S.M.A. Razzak, Tailoring polarization maintaining broadband residual dispersion compensating octagonal photonic crystal fibers, *Opt. Eng.* 52 (2013) 116111(1-8).
- [8] S.F. Kaijage, Y.N. A, N.H. Hai, F. Begum, Broadband Dispersion Compensating Octagonal Photonic Crystal Fiber for Optical Communication Applications, *Jpn. J. Appl. Phys.* 48 (2009) 052401(1-8).
- [9] M.A. Islam, M.A. Hossain, Broadband light source based on highly nonlinear non-circular core photonic crystal fiber for medical applications, *Opt. Laser Technol.* 44 (2012) 2476–2482.
- [10] P. Jamatia, T.S. Saini, A. Kumar, R.K. Sinha, Design and analysis of a highly nonlinear composite photonic crystal fiber for supercontinuum generation: visible to mid-infrared, *Appl. Opt.* 55 (2016) 6775–6781.
- [11] M.A. Hossain, Y. Namihira, M.A. Islam, Y. Hirako, Supercontinuum Generation at 1.55 um Using Highly Nonlinear Photonic Crystal Fiber for Telecommunication and Medical Applications, *Opt. Rev.* 19 (2012) 315–319.
- [12] J.M. Dudley, G. Genty, S. Coen, Supercontinuum generation in photonic crystal fiber, *Rev. Mod. Phys.* 78 (2006) 1135–1184.
- [13] X. Wang, D. Wang, X. Shen, Z. Wu, X. He, J. Yuan, X. Wang, C. Yu, Supercontinuum generation from ultraviolet and visible wavelength, *Optik*, 140 (2017) 423–426.
- [14] Q. Xu, Y. Zhao, M. Wang, Y. Zhang, B. Hao, Supercontinuum generation in highly nonlinear low-dispersion photonic crystal fiber, *Proc. SPIE.* 10250 (2017) .
- [15] A.A. Nair, S.K. Sudheer, M. Jayaraju, Design and Simulation of Octagonal Photonic Crystal Fiber for Supercontinuum Generation, *Adv. Opt. Sci. Eng. Proc. Phys.* 166. 166 (2015) 195–202.
- [16] M.M. Rashid, M.S. Anower, M.I. Hasan, M.R. Hasan, Highly Birefringent Octagonal Shaped Photonic Crystal Fiber with Two Zero Dispersion Wavelengths in Ti : sapphire Oscillator Range, *Proc. 3rd Int. Conf. onElectrical Eng. Inf. Commun. Technol.* 2016. (2016) 3–7.
- [17] M. Sharma, S. Konar, Broadband supercontinuum generation in lead silicate photonic crystal fibers employing optical pulses of 50W peak power, *Opt. Commun.* 380 (2016) 310–319.
- [18] M. Sharma, S. Konar, K.R. Khan, Supercontinuum generation in highly nonlinear hexagonal photonic crystal fiber at very low power, *J. Nanophotonics.* 9 (2015) 93073.